

# Guidance of vortices and the vortex ratchet effect in high- $T_c$ superconducting thin films obtained by arrangement of antidots

R. Wördenweber and P. Dymashevski

*Institut für Schichten und Grenzflächen (ISG) and cni-Center of Nanoelectronic Systems for Information Technology, Forschungszentrum Jülich, D-52425 Jülich, Germany*

V. R. Misko\*

*Institut für Schichten und Grenzflächen (ISG) and cni-Center of Nanoelectronic Systems for Information Technology, Forschungszentrum Jülich, D-52425 Jülich, Germany*  
*and Frontier Research System, The Institute of Physical and Chemical Research (RIKEN), Wako-Shi, Saitama 351-0198, Japan*  
 (Received 13 November 2003; revised manuscript received 11 February 2004; published 20 May 2004)

Controlled trapping and guided motion of vortices via special arrangements of microholes, so-called antidots, in  $\text{YBa}_2\text{Cu}_3\text{O}_7$  films and devices is demonstrated. Resistive Hall-type measurements prove the presence of guided flux motion along rows of antidots. In contrast to conventional vortex motion due to vortex unpinning at currents exceeding the critical current, this motion is present down to zero current and low temperatures. It is characterized by a linear voltage–current dependence, i.e., Ohmic behavior. The latter is indicative for a novel mechanism of vortex propagation that is probably based upon flux nucleation within antidots due to the redistribution of screening currents and flux quantization. Together with trapping of vortices by isolated antidots this mechanism can be used for new devices concepts. As an example a vortex ratchet formed by a special arrangement of antidots is demonstrated.

DOI: 10.1103/PhysRevB.69.184504

PACS number(s): 74.25.Fy, 74.72.Bk, 74.78.Na

## I. INTRODUCTION

Due to perspectives of application of nanostructures in micro- and nanoelectronics as well as to new insight in fundamental problems arising at boundaries or in low-dimensional systems, experimental and theoretical studies of nano- and mesoscopic systems represent one of the challenging present goals of research. In this context the understanding of vortex matter in mesoscopic patterned superconducting thin films has to be considered. Recent progress in fabrication of thin film nanostructures made it possible to fabricate complex superconducting samples with lateral extensions as small as 50 nm or large regular arrays consisting of practically identical nanostructures. Thus, analysis of the nucleation, penetration and dynamics of vortices in nanostructured superconductors has gained a lot of interest.<sup>1–9</sup> It already led to new insight into these processes, which are also relevant for the understanding of the behavior of any “extended” superconducting devices.

Furthermore, flux penetration has to be expected in most superconducting electronic devices designed for real applications. These devices usually contain superconducting areas with lateral extension of typically  $w \approx 100 \mu\text{m}$  up to even some mm. As a result, extremely small field values for tunneling penetration  $B_T = B_{c1} \cdot d/w$  and collective penetration  $B_P = B_{c1} \cdot (2d/w)^{1/2}$  are expected,<sup>10,11</sup> here  $B_{c1}$  and  $d$  represent the lower critical field and thickness of the film, respectively. Inserting typical parameters for high- $T_c$  material  $\text{YBa}_2\text{Cu}_3\text{O}_7$  (YBCO) [e.g.,  $d = 200 \text{ nm}$ ,  $B_{c1}(77 \text{ K}) \approx 8 \text{ mT}$ ] the situation  $B_T < B_{\text{earth}} < B_P$  is encountered for most devices. Thus, single vortices tunnel into typical superconducting devices that are exposed to an earth field  $B_{\text{earth}}$ . It is known, that the presence and the motion of these vortices will lead to a degradation of the properties of active<sup>12,13</sup> and passive<sup>14</sup> devices.

In this paper both aspects will be combined, i.e., it is shown, that mesoscopic structures in extended superconducting areas can be utilized for the control of the vortex penetration and motion. It is demonstrated, that adequate arrangements of mesoscopic holes (antidots) lead to (i) flux trapping and/or (ii) guided motion of vortices. Both effects—trapping and guided motion—can be of advantage for the optimization of existing superconducting devices as well as for the conception of new devices, e.g., a vortex ratchets effect is demonstrated in this work.

One of the most effective ways to create artificial pinning sites in thin films is provided by the preparation of antidots.<sup>15–18</sup> These defects can be placed arbitrarily in superconducting thin film devices and, in contrast to other pinning defects, that have to be of the size of the superconducting coherence length  $\xi$ , holes with sizes much larger than  $\xi$  will trap flux very effectively.<sup>17,18</sup> It has been demonstrated that antidots of sizes down to 250 nm in diameter can be patterned into YBCO thin films and thin film devices without deterioration of the superconducting and device properties, respectively.<sup>17–19</sup> Moreover, commensurability effects demonstrate the attractive interaction between vortices and antidots, and reduction of the low frequency noise of SQUIDs in ambient magnetic fields is achieved by a few, “strategically well positioned” antidots in the superconducting device, which trap only those vortices, that attribute strongly to the low-frequency noise. However, although vortex trapping by isolated antidots has been shown, it is not clear whether and how flux can move between antidots. Moreover, the question remains, whether flux can be guided by artificial defects, e.g., rows of antidots.

## II. RESULTS AND DISCUSSION

The guidance of vortices via rows of antidots is measured resistively via 4-probe Hall-type experiments. The YBCO

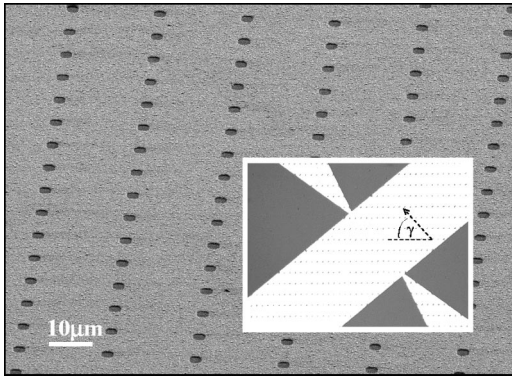


FIG. 1. SEM image of a typical arrangement of an antidot lattice. The inset shows the Hall contacts for a sample with rows of antidots arranged with an angle  $\gamma = -35^\circ$  with respect to the Lorentz force.

thin films (thickness of 100–150 nm) are deposited on  $\text{CeO}_2$  buffered sapphire via magnetron high-pressure sputtering technology. For protection and improvement of the lithography, the YBCO films are covered with a 50 nm thick Au layer. The antidots lattices are patterned via optical lithography and the ion beam etching. Details of the preparation are given in Refs. 17–19. Figure 1 shows a typical arrangement of an antidots lattice (lattice periodicities:  $10 \mu\text{m} \times 20 \mu\text{m}$ , antidot radius:  $1 \mu\text{m}$ ) in a Au-shunted YBCO film and, in the inset, of the Hall contacts. The angle  $\gamma$  is defined by the directions of Lorentz force  $F_L$  with respect to the orientation of the rows of antidots.

A typical set of  $IV$  characteristics of the Hall-type measurements are shown in Fig. 2. At temperature  $T > T_c$  Ohmic behavior is observed over the complete current range. A small (in this case positive) Hall resistance is measured that can be ascribed to the positive Hall effect for YBCO or slight misalignments of the contacts (it should be noted that the samples are shunted with a 50 nm thin Au layer for protection). A more complicated behavior is observed for temperatures  $T < T_c$ . In spite of the superconducting state, Ohmic behavior is present up to a characteristic current, at which a nonlinear behavior sets in.<sup>20</sup> Simultaneous flux-flow measurements in standard four-probe measurements demonstrate, that these characteristic current values coincide with the onset of flux flow in the superconductor at the critical current  $I_c$ . Since  $I_c$  increases with decreasing temperature, the nonlinearity is only displayed in Fig. 2(a) for temperatures close to  $T_c$ .

In the first part, we will focus our discussion on the unusual linear behavior observed for small applied currents  $|I| < I_c$ . This current regime is characterized by a finite Ohmic Hall resistance  $R_H = dV_{\text{Hall}}/dI$ . Figures 2(b) and 2(c) show the temperature dependence of  $R_H$ . Below  $T_c$  a sharp minimum is present, followed by an increase of  $R_H$ . Further reduction of the temperature leads to a second pronounced reduction of the Hall resistance, which levels off below 85 K. The first part of this curve resembles the anomalous Hall effect that is usually observed in high- $T_c$  material (HTS),<sup>21,22</sup> which is indicated by the dashed line in Fig. 2(c). That is, in the reversible regime for temperatures close to  $T_c$ , flux flow

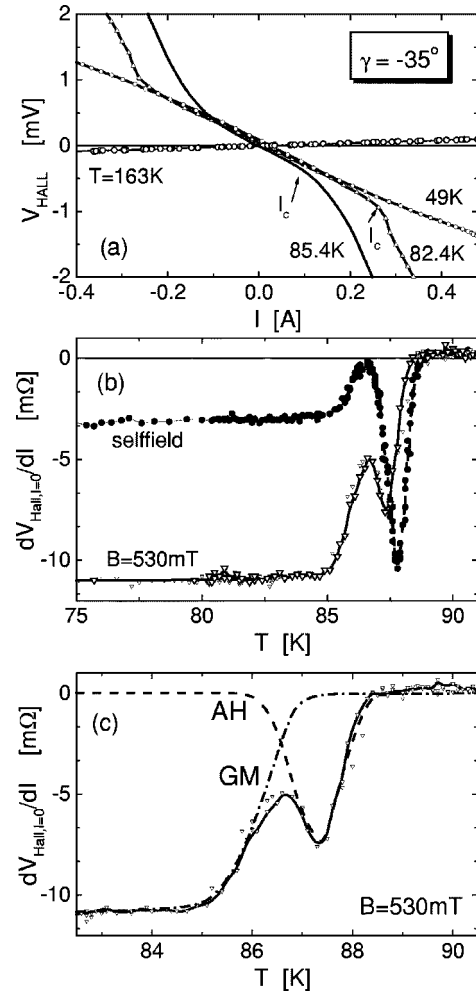


FIG. 2. (a) Hall voltage as a function of the applied current for different temperatures, self-field and  $\gamma = -35^\circ$ , (b) the resulting temperature dependence of the Hall resistance of the sample at zero-current for different magnetic fields, and (c) sketch of the two different components of the Hall resistance [anomalous Hall effect (AH) and guided motion (GM)] for the data obtained at 530 mT. The YBCO film thickness of this sample is 200 nm.

leads to a negative Hall coefficient  $R_{HC} = (dV/dI) \cdot (d/B)$  in HTS.  $B$  represents the applied magnetic field,  $d$  is the thickness of the superconducting film. However, below the irreversibility line [at about 87.2 K for the case illustrated in Fig. 2(c)] the anomalous Hall coefficient rapidly approaches zero.

Thus, the second reduction of the measured Hall resistance [below about 86.5 K for the case illustrated in Fig. 2(c)] cannot be explained in terms of the anomalous Hall effect. Moreover, reference measurements on samples without antidots as well as temperature-dependent measurements of the Hall resistance for different angles  $\gamma$  (see Fig. 3) clearly indicate, that at low temperatures  $T < 83$  K the Hall resistance is determined by the direction of vortex motion guided by the rows of antidots. Figure 3 displays negative, zero and positive Hall resistances measured at low temperatures for  $\gamma < 0$ ,  $\gamma = 0$  and  $\gamma > 0$ , respectively. The sketch in Fig. 3(c) illustrates the angular dependence of  $R_H$  given in a simplified 1-channel model, in which the flux is expected to drift predominantly along the row of antidots. The compo-

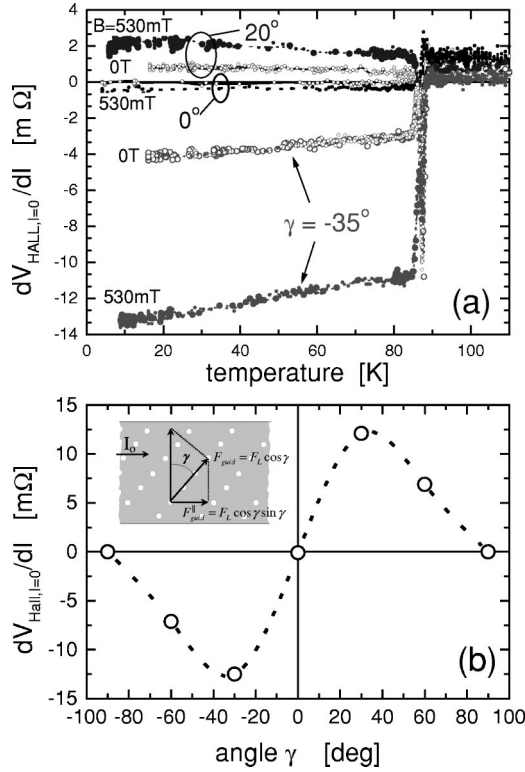


FIG. 3. (a) Temperature dependence of the Hall resistance for different orientations  $\gamma = 20^\circ$ ,  $0$  and  $-35^\circ$  and magnetic fields (self-field and 530 mT), (b) angular dependence of  $R_H$  measured on circular shaped 90 nm thick sample at 30 K, 143 mT with a current amplitude of 10 mA, and (inset) schematic illustration of the angular dependence of  $R_H$ .

ment of the Lorentz force, which compels vortices to move along the antidot rows (i.e., guided motion), is  $F_{\text{guid}} = F_L \cos \gamma$ , where  $F_L$  is the modulus of the Lorentz force:  $F_L = |\mathbf{F}_L|$ . In its turn, it is the component of  $F_{\text{guid}}$  parallel to the applied current,

$$F_{\text{guid}}^{\parallel} = F_{\text{guid}} \sin \gamma = F_L \cos \gamma \sin \gamma, \quad (1)$$

which contributes to the Hall voltage and leads to Hall resistance  $R_H \propto F_L \cos \gamma \sin \gamma$ . The experimentally determined angular dependence of  $R_H$  shown in Fig. 3(b) roughly obeys this simple relation obtained in this “1-channel model.” Actually, it has to be considered, that vortices can move with some probability also between antidots of neighboring rows. These additional channels of vortex motion become important for angles  $\gamma$  close to  $90^\circ$  [Fig. 3(c)]. However, for these values of  $\gamma$  the contribution of the vortex motion to  $R_H$  is small [see Eq. (1)]. Nevertheless, taking into account these additional channels of vortex motion (i.e., vortices motion between antidots of adjacent rows), Eq. (1) should be substituted by a more general expression yielding

$$R_H \propto \sum_i P_i(\gamma) F_L \cos \gamma \sin \gamma, \quad (2)$$

where summation is performed over all the channels of vortex motion, and  $P_i(\gamma)$  is the angle-dependent probability of the motion along the  $i$ th channel.

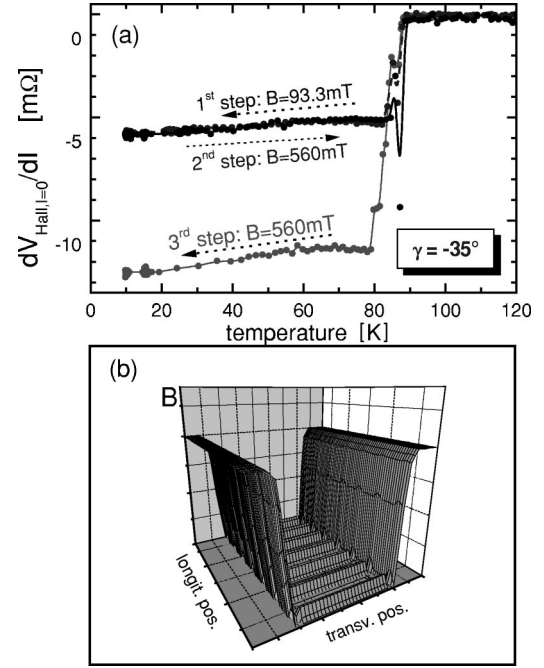


FIG. 4. (a) Memory effect observed in field-sweep experiments. Starting with a small field  $B = 93.3$  mT the field is changed at low temperature  $T = 10$  K, heated up to  $T > T_c$  and cooled down again. The measurement is executed with current amplitudes clearly smaller than  $I_c$  for  $T < 80$  K. The panel (b) represents a schematic sketch of the flux density distribution of the stripline after the field change at low temperature. Longitudinal and transversal directions denote the directions along and across the stripline, respectively.

A second interesting feature of the Hall resistance due to guided vortex motion is revealed by field sweep measurements. Although  $R_H$  strongly depends on the magnetic field (see Fig. 3), it is the frozen-in field that matters. A change of the magnetic field at low temperatures  $T < T_{\text{irr}}$  does not affect the Hall resistance at all. This is demonstrated in field-sweep experiments shown in Fig 4. During warming up,  $R_H$  follows exactly the data of the cooling down curve in Fig. 4(a). Only after transition to the normal state the Hall voltage is modified, which is visible in the second cooling down. This observation confirms the presence of two independent flux-flow mechanisms, which had already been indicated by the linear and nonlinear part of the Hall-type  $IV$  curves for  $\gamma \neq 0$ .

#### A. Flux motion for $I < I_c$

At small currents  $I < I_c$  (and in the irreversible regime,  $T < T_{\text{irr}}$ ), flux propagates along the rows of antidots. Amazingly, this type of motion is not restricted to a threshold, i.e., no finite barrier is impeding this motion. Thus, flux seems not to shuttle from antidot to antidot similarly to the “classical” motion of an individual vortex in a superconductor. This classical mechanism of vortex motion is subject to dissipation and pinning due to the vortex–pin and the vortex–vortex interactions and, therefore, characterized by a critical current density and a flux-flow resistance that decreases with decreasing temperature. Both characteristics are not present for out case and  $I < I_c$  (the critical current characterizing the onset of classical flux motion within the superconductor it-

self), i.e., Ohmic and, thus, no critical behavior is measured at low currents values [see Fig. 2(a)] and the absolute value of the Hall resistance increases with decreasing temperature [see Fig. 3(a)].

In the low current density regime, flux motion seems to be of a different nature. Various scenarios can be envisaged that are principally based on (a) the size restriction of the area, in which the vortex is nucleated, or/and (b) the redistribution of the screening current of flux in the antidots at adjacent holes.

Flux motion across a superconducting microbridge of the size of the characteristic length of the superconductor will not lead to vortex formation. A phase slip line will develop along the path of the flux motion leading to Josephson-type behavior of the bridge. In this case a pinning of the traveling flux is not possible. According to theory the characteristic length of the superconductor for this effect should be the coherence length  $\xi$ . However, it has been shown that phase slip lines are present for bridge dimensions  $w$  up to the penetration length  $\lambda$ .<sup>23</sup> In fact, the effective penetration length  $\lambda_{\text{eff}}(T) = \lambda_L(T) \coth\{d/2\lambda_L(T)\}$  in our samples (YBCO with London penetration length  $\lambda_L(4\text{ K}) = 180\text{--}200\text{ nm}$  and thickness  $d = 90\text{--}150\text{ nm}$ ) range between 500 and 900 nm. Furthermore, for HTS thin films it has been shown, that phase slip can be present even in bridges with dimensions up to  $w = 1\text{--}1.5\ \mu\text{m} \gg \lambda$ .<sup>24</sup>

Another interesting effect that might have relation to the motion of vortices (e.g., driven by an applied current) in mesoscopic systems is known from observations of von Karman vortices. After nucleation the vortex structure develops in time. Due to the motion a given space is necessary for a vortex to fully develop. If this space is not provided, vortices will not be originated. A similar situation might apply for Abrikosov vortices in mesoscopic superconductors. The nucleation of flux in the superconductor and its shuttling between adjacent antidots might not lead to vortex formation due to the restricted distance between the antidots.

Additionally, the impact of the distribution of screening currents in patterned superconductors has to be considered. The distribution of the screening current can be obtained by solving the Ginzburg–Landau (GL) equations for the order parameter  $\psi$  and the vector potential  $\mathbf{A}$  of a magnetic field  $\mathbf{H} = \nabla \times \mathbf{A}$ ,<sup>25,26</sup> which can be presented in the dimensionless form as follows:

$$\begin{aligned} (-i\nabla - \mathbf{A})^2 \psi - \psi \left[ \left( 1 - \frac{T}{T_c} \right) - |\psi|^2 \right] &= 0, \\ \kappa^2 \Delta \mathbf{A} &= \frac{i}{2} (\psi^* \nabla \psi - \psi \nabla \psi^*) + \mathbf{A} |\psi|^2, \end{aligned} \quad (3)$$

with the imposed boundary condition,

$$\mathbf{n} \cdot (-i\nabla \psi - \mathbf{A} \psi)|_{\text{boundary}} = 0. \quad (4)$$

In Eqs. (3)–(4),  $\mathbf{n}$  is the unit vector normal to the boundary,  $\kappa = \lambda(T)/\xi(T)$ , and  $T_c$  is the critical temperature. Then the superconducting current is obtained from the second GL equation:

$$\mathbf{j} = -\kappa^2 \nabla^2 \mathbf{A}. \quad (5)$$

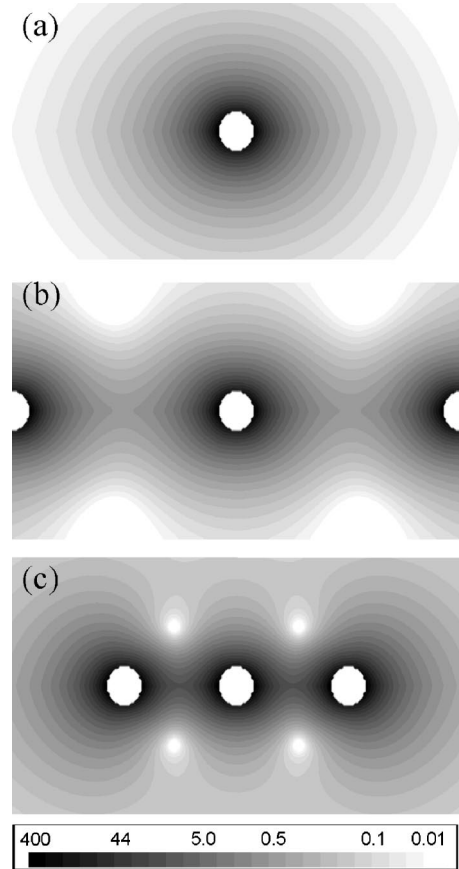


FIG. 5. Density distribution of the screening current for two-dimensional superconductor (e.g., thin film) with a row of antidots placed at different distances  $d_v$  (measured in units of the antidot radius) from each other obtained from simulations on the basis of the Ginzburg–Landau equations in the high- $\kappa$  limit: (a)  $d_v = 66.7$ , (b)  $d_v = 13.3$ , (c)  $d_v = 6.7$ . High local current densities are indicated with dark gray, the scale is given in arbitrary units.

In order to analyze the interplay of the screening currents of trapped flux created at neighboring antidots, the current distributions have been calculated in a model of an infinite (in-plane) superconductor characterized by the GL parameter  $\kappa = 95$ , which is typical value for YBCO,<sup>27</sup> containing few cylindrical-shaped antidots (holes) placed at different distances  $d_v$  from each other. The antidot spacing  $d_v$  is given in units of the antidot radius. The results of the calculations are shown in Fig. 5 for the system of three antidots. In the case of an isolated antidot and in the absence of external current, the screening current is distributed symmetrically around the antidot. As expected the distribution shows a maximum near the antidot boundary and decreases with increasing radial distance from the antidot according to  $j = j_0 \exp(-r/\lambda)$ . However, the symmetric current pattern is immediately distorted by presence of other screening currents produced by additional antidots even if they are placed at rather long distances [Fig. 5(a)]. Moreover, if the antidot–antidot spacing decreases, the screening currents start to overlap stronger [Fig. 5(b)] and start to form a *closed loop* of the current flowing around a complete row of antidots [Fig. 5(c)]. The appearance of this common screening current for the complete row of antidots and the fluxoid quantization condition

leads to an easy transport mechanism of the flux between adjacent antidots at  $I < I_c$ . The redistribution of the current that screens the quantized magnetic flux  $n\Phi_0$  contained in the adjacent antidot will automatically lead to induced magnetic flux  $\Phi_i$  at adjacent antidots. Depending on the energy balance, flux quantization will either cause suppression of this extra flux or cause compensation via nucleation of an additional flux quantum at the antidot. The geometry of the experimental is best described for  $d_v \approx 10$  in the simulation. Thus, a relatively large common screening current of the rows of antidots and easy flux transfer between adjacent antidots has to be expected in the experiment according to the calculations. The results of the simulations are comparable to predictions of so called kinematic vortices in the literature, which are obtained by numerical simulations using two-dimensional time-dependent Ginzburg–Landau equations.<sup>28</sup> Furthermore, it can be speculated that this mechanism of flux transfer potentially leads to unusually high vortex mobility and might be of interest for a number of rf application (e.g., rf flux-flow transformer).

### B. Flux motion for $I > I_c$

The finite critical current  $I_c$  defines the onset of depinning of vortices in the superconducting matrix. It was determined via standard 4-probe-flux-flow measurements. The measured critical current densities agree with literature values, e.g.,  $J_c(77\text{ K}) = 1\text{--}2\text{ MA cm}^{-2}$ . As long as currents  $I < I_c$  are applied, the vortex density (and, thus, magnetic flux) in the superconductor itself (not in the antidots) is unaltered. This situation explains the memory effect observed in field-sweep experiments (see Fig. 4). Thus, the magnetic flux density frozen into the superconducting matrix determines the amount of flux transported along the rows of antidots via mechanism (i). The memory effect might also be interesting for a number of applications.

Finally, it is shown that trapping and guided motion of vortices via antidots might lead to new device concepts. As an example, a vortex ratchet test structure is patterned and characterized. The special arrangement of the antidots is sketched in the inset of Fig. 6. Rows of antidots are oriented with an angle  $\gamma = -45^\circ$  with respect to the driving Lorentz force. Additionally, pairs of antidots forming a “dead end” with angle  $\gamma = 0$  are repeatedly attached to the rows. Applying an ac current with amplitude  $I < I_c$  leads to a unsymmetrical Hall response at low temperatures (see Fig. 6) that can be ascribed to the guidance and trapping of this arrangement. For small relative current amplitudes  $I/I_c \ll 1$  at low temperatures a plateau is present in the positive voltage branch indicating the effect of the vortex trapping in the “dead ends” of the antidot structure. These experiments should be considered as proof of the principle only. The unsymmetrical response is clearly visible but not very pronounced. Experiments at higher frequencies (our experimental range was restricted to 150 kHz) or/and improvement of the devices design might lead to a more pronounced ratchet effect.

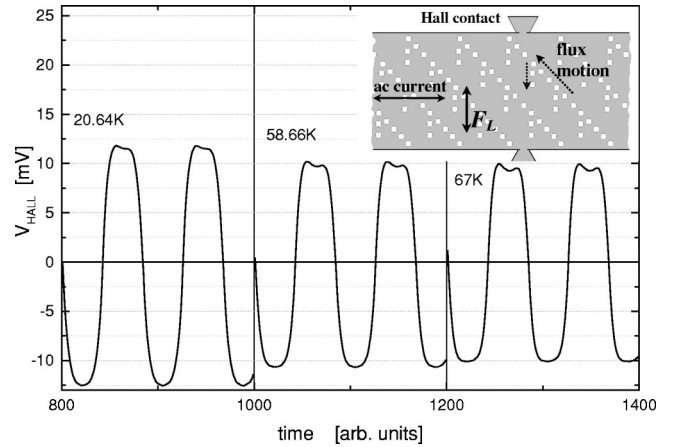


FIG. 6. Demonstration of vortex ratchet effect and (inset) schematic drawing of the arrangements of antidots. The main panel displays the recorded Hall voltage resulting from a sinusoidal ac driving current (frequency: 511 Hz, amplitude: 10 mA) at three different temperatures.

### III. CONCLUSION

In conclusion, trapping and guided motion of vortices via special arrangements of antidots in YBCO films and devices is demonstrated. Resistive Hall-type measurements prove the presence of guided flux motion along rows of antidots. In contrast to conventional vortex motion due to vortex unpinning at currents  $I > I_c$ , this motion is present down to zero current even down to low temperatures  $T = 4\text{ K}$ . It is characterized by a linear voltage–current dependence (Ohmic behavior). This is indicative for a novel mechanism of flux propagation in superconducting systems that might be based upon (a) restricted vortex formation in mesoscopic superconductors or/and (b) flux nucleation within antidots due to the redistribution of screening currents. The combination of strategically trapping of vortices and guided vortex motion using isolated or rows of antidots, respectively, can be used for new device concepts. As a first example a test structure of a vortex ratchet formed by a special arrangement of antidots has been shown. The experiments demonstrate the unique possibilities of artificial defects in superconducting devices employed in little- or unshielded environment. The analysis of the mechanism of flux motion in these mesoscopically patterned superconducting systems might lead to new, interesting insight into the colorful physics of vortex matter.

### ACKNOWLEDGMENTS

Discussions with H. P. Bochem, S. Bunte, A. Castellanos, W. Hofer, E. Hollmann, R. Kutzner, N. Klein, R. Kleiner, D. Koelle, P. Lahl, R. Ott, and V. Yurchenko are acknowledged. This work was supported by DFG Grant No. WO549/3-1 and the ESF Program VORTEX. V.R.M. acknowledges the “Short Term Fellowship” of the ESF Program VORTEX.

\*On leave from Institute of Applied Physics, str. Academiei 5, MD-2028 Kishinev, Republic of Moldova.

- <sup>1</sup>V. V. Moshchalkov, L. Gielen, C. Strunk, R. Jonckheere, X. Qiu, C. Van Haesendonck, and Y. Bruynseraede, *Nature (London)* **373**, 319 (1995).
- <sup>2</sup>V. M. Fomin, V. R. Misko, J. T. Devreese, and V. V. Moshchalkov, *Solid State Commun.* **101**, 303 (1997); *Phys. Rev. B* **58**, 11703 (1998).
- <sup>3</sup>M. Poza, E. Bascones, J. G. Rodrigo, N. Agraït, S. Vieira, and F. Guinea, *Phys. Rev. B* **58**, 11173 (1998).
- <sup>4</sup>V. R. Misko, V. M. Fomin, and J. T. Devreese, *Phys. Rev. B* **64**, 014517 (2001).
- <sup>5</sup>P. Singha Deo, V. A. Schweigert, F. M. Peeters, and A. K. Geim, *Phys. Rev. Lett.* **79**, 4653 (1997).
- <sup>6</sup>V. A. Schweigert, F. M. Peeters, and P. Singha Deo, *Phys. Rev. Lett.* **81**, 2783 (1998).
- <sup>7</sup>V. A. Schweigert and F. M. Peeters, *Phys. Rev. Lett.* **83**, 2409 (1999).
- <sup>8</sup>V. R. Misko, V. M. Fomin, J. T. Devreese, and V. V. Moshchalkov, *Physica C* **369**, 361 (2002).
- <sup>9</sup>V. R. Misko, V. M. Fomin, J. T. Devreese, and V. V. Moshchalkov, *Phys. Rev. Lett.* **90**, 147003 (2003).
- <sup>10</sup>E. Zeldov, A. I. Larkin, V. B. Geshkenbein, M. Konczykowski, D. Majer, B. Khaykovich, V. M. Vinokur, and H. Shtrikman, *Phys. Rev. Lett.* **73**, 1428 (1994).
- <sup>11</sup>R. Clem (unpublished).
- <sup>12</sup>P. Selders and R. Wördenweber, *Appl. Phys. Lett.* **76**, 3277 (2000).
- <sup>13</sup>R. Wördenweber and P. Selders, *Physica C* **366**, 135 (2002).
- <sup>14</sup>P. Lahl and R. Wördenweber, *Appl. Phys. Lett.* **81**, 505 (2002).
- <sup>15</sup>M. Baert, V. V. Metlushko, R. Jonckheere, V. V. Moshchalkov, and Y. Bruynseraede, *Phys. Rev. Lett.* **74**, 3269 (1995).
- <sup>16</sup>A. N. Lykov, *Solid State Commun.* **86**, 531 (1993).
- <sup>17</sup>A. M. Castellanos, R. Wördenweber, G. Ockenfuss, A. v.d. Hart, and K. Keck, *Appl. Phys. Lett.* **71**, 962 (1997).
- <sup>18</sup>R. Wördenweber, A. M. Castellanos, and P. Selders, *Physica C* **332**, 27 (2000).
- <sup>19</sup>P. Selders, A. M. Castellanos, M. Vaupel, and R. Wördenweber, *Appl. Supercond.* **5**, 269 (1998).
- <sup>20</sup>It should be noted, that a small Ohmic contribution is also present in the 4-probe measurements of the restive response measured along the current direction. As explained later, this contribution is caused by the guided motion of flux. This contribution is small compared to the flux-flow contribution, that sets in at  $I_c$ , where the majority of vortices in the superconductor itself become unpinned and move in the direction of the Lorentz force.
- <sup>21</sup>W. Lang, W. Göb, J. D. Pedarnig, R. Rössler, and D. Bäuerle, *Physica C* **364-365**, 518 (2001).
- <sup>22</sup>It should be noted, that the positive Hall coefficient usually observed for  $T > T_c$  is reduced by an Au-top layer, that is used for the patterning and protection of the YBCO film.
- <sup>23</sup>K. K. Likharev and L. A. Yakobson, *Sov. Phys. Tech. Phys.* **20**, 950 (1976).
- <sup>24</sup>J. Schneider, H. Kohlstedt, and R. Wördenweber, *Appl. Phys. Lett.* **63**, 2426 (1993); J. Schneider, M. Mück, and R. Wördenweber, *ibid.* **65**, 2475 (1994); A. G. Sivakov, A. M. Glukhov, A. N. Omelyanchouk, Y. Koval, P. Müller, and A. V. Ustinov, *Phys. Rev. Lett.* **91**, 267001 (2003).
- <sup>25</sup>V. L. Ginzburg and L. D. Landau, *Zh. Eksp. Teor. Fiz.* **20**, 1064 (1950).
- <sup>26</sup>M. Tinkham, *Introduction to Superconductivity*, 2nd ed. (McGraw-Hill, New York, 1996).
- <sup>27</sup>C. P. Poole, Jr., H. A. Farach, and R. J. Creswick, *Superconductivity* (Academic, San Diego, 1995), p. 271.
- <sup>28</sup>A. Andronov, I. Gordion, V. Kurin, I. Nefedov, and I. Shereshevsky, *Physica C* **213**, 193 (1993).